Biofilm 9 (2025) 100254

Contents lists available at ScienceDirect

Biofilm

journal homepage: www.sciencedirect.com/journal/biofilm

Integration of BrfS into the biofilm-controlling cascade promotes sessile *Salmonella* growth at low temperatures

Gonzalo Tulin [a], Andrea A.E. Méndez [a], Nicolás R. Figueroa [a,e], Carol Smith [b], María P. Folmer [a], Diego Serra [a], Joseph T. Wade [b,c,d], Susana K. Checa [a], Fernando C. Soncini [a,*]

[a] *Instituto de Biología Molecular y Celular de Rosario, Facultad de Ciencias Bioquímicas y Farmacéuticas, Universidad Nacional de Rosario, Consejo Nacional de Investigaciones Científicas y Técnicas, Rosario, Argentina*
[b] *Wadsworth Center, New York State Department of Health, Albany, NY, USA*
[c] *Department of Biomedical Sciences, School of Public Health, University at Albany, Albany, NY, USA*
[d] *RNA Institute, University at Albany, SUNY, Albany, NY, USA*
[e] *Current position: Centro de Estudios Fotosintéticos y Bioquímicos, Consejo Nacional de Investigaciones Científicas y Técnicas, Rosario, Argentina*

ARTICLE INFO

Keywords:
Salmonella
Biofilm transcriptional control
MlrA-homolog
Extracellular matrix
Low-temperature

ABSTRACT

Biofilm formation is stimulated by different stress-related physiological and environmental conditions. In *Salmonella* and *Escherichia coli*, curli fibers and phosphoethanolamine-cellulose are the major extracellular components of biofilms. The production of both is under the control of CsgD, a transcriptional regulator whose expression is modulated by a number of factors responding to different signals. The atypical MerR-like regulator MlrA is key in the activation of *csgD* transcription in both *Salmonella* and *E. coli*. Recently, MlrB, a SPI-2-encoded MlrA-like regulator that counteracts MlrA by repressing *csgD* transcription and biofilm formation inside macrophages was identified. Here, we characterize STM1266, a *Salmonella*-specific MlrA-like regulator, recently renamed BrfS. In contrast to *mlrA*, *brfS* transcription increases in minimal growth media and at 20 °C, a temperature not commonly tested in laboratories. Under these conditions, as well as in salt-limited rich medium, deletion or overexpression of *brfS* affects extracellular matrix production. Using transcriptomics, we uncovered genes under BrfS control relevant for biofilm formation such as *csgB* and *bapA*. Transcriptional analysis of these genes in mutants lacking *brfS*, *csgD* or both, indicates that BrfS controls curli biosynthesis both in a CsgD-dependent and independent manner. By contrast, at low temperatures, *bapA* transcription depends only on BrfS, and neither deletion of *csgD* nor of *mlrA* modify its expression. Based on these results, we propose that BrfS contributes to *Salmonella* persistence in the environment, where the pathogen encounters low temperatures and nutrient limitation.

1. Introduction

Salmonella is the causative agent of a variety of infections, from self-limited gastroenteritis to life-threatening Typhoid fever [1]. In addition, it has a remarkable capability to adapt its lifestyle to different intra- and extra-host conditions [2–4]. *Salmonella* is usually acquired by ingestion of contaminated water or food [5]. A key aspect that contributes to *Salmonella* persistence in both the environment and the host is its ability to form biofilms, an assemblage of tightly associated bacteria embedded in a self-produced matrix [6]. The *Salmonella* extracellular matrix can include diverse components such as amyloid fibers known as "curli" [7,8], the surface protein BapA [9], exopolysaccharides such as phosphoethanolamine-cellulose (pEtN-cellulose) [10], colanic acid [11] and O-antigen [12], and extracellular DNA [13]. Although the specific composition of biofilms varies depending on the particular environment that the bacteria are encountering, curli and pEtN-cellulose are the major components detected and are primarily responsible for the spatial configuration of biofilms in both *Escherichia coli* and *Salmonella* under laboratory conditions [14,15].

The structural and regulatory components of curli are encoded in two divergent operons on the *Salmonella* chromosome, *csgBAC-csgDEFG* [8,16]. These genes are also found in several Enterobacteriaceae species such as *E. coli*, *Shigella*, *Enterobacter*, and *Citrobacter* [17,18]. The *csgBAC* operon encodes CsgA and CsgB, the major and minor structural subunits

* Corresponding author.
E-mail address: soncini@ibr-conicet.gov.ar (F.C. Soncini).

https://doi.org/10.1016/j.bioflm.2025.100254
Received 16 July 2024; Received in revised form 14 January 2025; Accepted 15 January 2025
Available online 21 January 2025

of the curli fiber, respectively [19]. The operon also encodes CsgC, a protein that prevents CsgA polymerization within the periplasm [20]. The *csgBAC* operon is transcriptionally controlled by CsgD, encoded in the opposite operon together with genes involved in curli transport and secretion [16,21]. CsgD also induces transcription of *adrA* and, at least in *S. enterica* serovar Enteritidis, the *bap* operon, which encodes the large surface protein BapA [9,16]. AdrA is a diguanylate cyclase (DGC) that stimulates pEtN-cellulose synthesis [16,22]. Thus, by regulating the synthesis of two key extracellular components both directly and indirectly, CsgD promotes biofilm formation. CsgD also modulates O-antigen capsule formation, essential for desiccation tolerance on abiotic surfaces [23].

CsgD is considered a regulatory hub that controls the transition of *Salmonella* between the motile (planktonic) and sessile (biofilm) lifestyles. Therefore, CsgD expression is tightly regulated by several factors, including the alternative sigma factor RpoS, and the atypical MerR-like regulator MlrA [24–26]. RpoS is responsible for the control of stationary phase adaptation, modulating the transcription of genes required for general stress responses [27]. In *E. coli*, MlrA activity is modulated by its interaction with specific enzymes, phosphodiesterases and diguanylate cyclases, that control the intracellular levels of the second messenger bis-(3′–5′)-cyclic dimeric GMP (c-di-GMP) [28]. Besides MlrA, *E. coli* produces BluR, a MlrA-like repressor that controls the production of colanic acid and downregulates curli synthesis at low temperatures [29,30].

Salmonella lacks BluR, but has two additional MlrA-like regulators, MlrB and STM1266 [31]. MlrB, encoded in the *Salmonella* pathogenicity island 2 (SPI-2), has an N-terminal DNA binding domain that shares 40 % identity with that of MlrA (Fig. 1). Unlike MlrA, MlrB represses the transcription of *csgD* [32]. This in turn prevents pEtN-cellulose production when *Salmonella* resides inside macrophages, allowing bacterial replication in the intracellular niche, a crucial step for the progression of the infection [33]. STM1266 is a more distant homolog of MlrA, MlrB, and BluR (Fig. 1A), even though they share several conserved amino acid residues, mainly at their N-terminal, DNA-binding domain (Fig. 1B). Kao et al. [34] recently reported that STM1266 affects curli synthesis and biofilm formation in liquid static cultures grown at 25 °C, as well as survival in mouse spleen. They named it BrfS (for biofilm regulator for *Salmonella*). However, BrfS regulatory targets or its activating conditions remained unexplored.

In this work, we analyze the environmental conditions that favor BrfS expression, identify its target genes, and evaluate its integration into the biofilm stimulon that modulates matrix production in *Salmonella*. We show that *brfS* transcription increases in minimal media and at low temperatures. In these conditions, not usually tested in *Salmonella,* BrfS induces transcription of the major curli components and *bapA*, even in the absence of CsgD. These results suggest that BrfS is required for *Salmonella* biofilm formation and persistence in the environment.

2. Results

2.1. brfS transcription increases in minimal media and at low temperatures

MlrA and MlrB control *csgD* transcription to modulate biofilm formation, responding to different environments [24,32]. Given the homology of BrfS to MlrA and MlrB (Fig. S1), we investigated the conditions that favor *brfS* expression. We generated a *S.* Typhimurium 14028s derivative carrying a chromosomal *lacZ*-transcriptional fusion to the *brfS* promoter, which we used in β-galactosidase activity assays, including a similar *mlrA:lacZ* strain as a control. β-galactosidase activity was determined in extracts from cells of both strains grown either in minimal (M9) media with glucose or in rich, low-salt, Lysogenic–Broth media (SLB) at different temperatures. The profile of *brfS* expression clearly differed from that of *mlrA* (Fig. 1). *brfS* expression increased as temperature decreased in both M9 and SLB. Nutrient limitation also

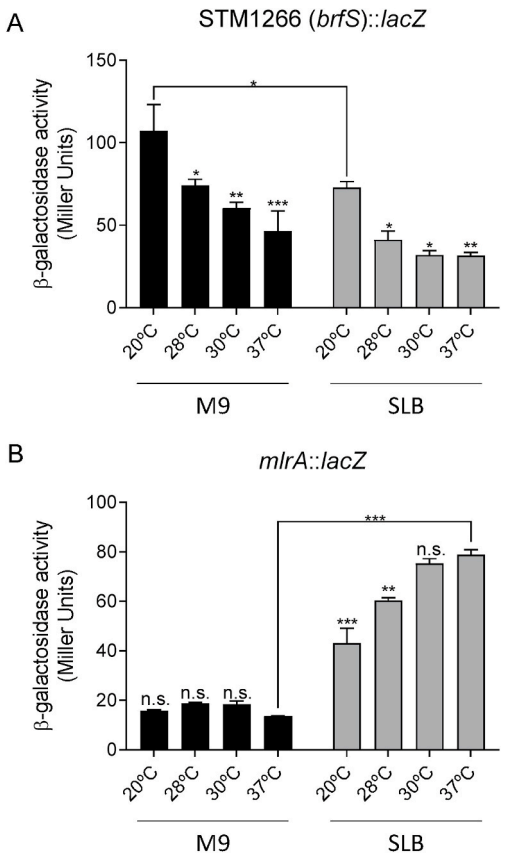

Fig. 1. Temperature-dependent expression of STM1266 (*brfS*) and *mlrA*. β-galactosidase activity was determined in extracts from STM1266 (*brfS*)*lacZ* (A) or *mlrA*:*lacZ* (B) cells grown overnight in either M9 or SLB media at 20 °C, 28 °C, 30 °C or 37 °C. The data correspond to an average of three independent experiments carried out by duplicate and the error bars represent *SD*. Symbols above the bars denote statistical significance relative to the temperature of maximal expression of each reporter in each condition: 20 °C for *STM1266 (brfS)lacZ* and 37 °C for *mlrA:lacZ*. Statistical significances were determined within each condition tested, and additionally, between the indicated bars. n. s., not significant; *, $p < 0.05$; **, $p < 0.01$; ***, $p < 0.001$.

favors *brfS* expression (Fig. 1A). By contrast, *mlrA* expression was higher in rich media than in minimal media, and increased at higher temperatures (Fig. 1B). These data suggest that BrfS functions primarily at low temperatures and in nutrient-deprived conditions.

2.2. BrfS stimulates biofilm formation at low temperatures

BrfS was previously shown to affect curli production and hence biofilm formation at the air/liquid interface after 7 days of incubation in static liquid rich media at 25 °C [34]. Deficiencies in curli production or unbalanced biofilm formation can be evidenced by growing the cells in SLB plates supplemented with Coomassie Blue and Congo Red dyes, known as CR plates [18]. We compared biofilms formed by either the wild-type (14028s) or the Δ*brfS* mutant strain under different experimental setups (Fig. 2). At 28 °C, deletion of *brfS* produced minor effects on either extracellular matrix production in liquid medium or on the colony morphotype on CR plates (Fig. 2A and B). Remarkably, wild-type strain biofilm formation is significantly enhanced at 20 °C compared to 28 °C. Colonies on CR plates were large and wrinkled (Fig. 2A), and exhibited the typical *rdar* (red, dry and rough) morphotype, indicative of a balanced increment in both curli and pEtN-cellulose in the extracellular matrix [18]. Growth at 20 °C also resulted in an increased biomass adhered to borosilicate beakers in static liquid cultures (Fig. 2B and C and Fig. S2 A-D). Moreover, the Δ*brfS* strain formed slightly smaller and

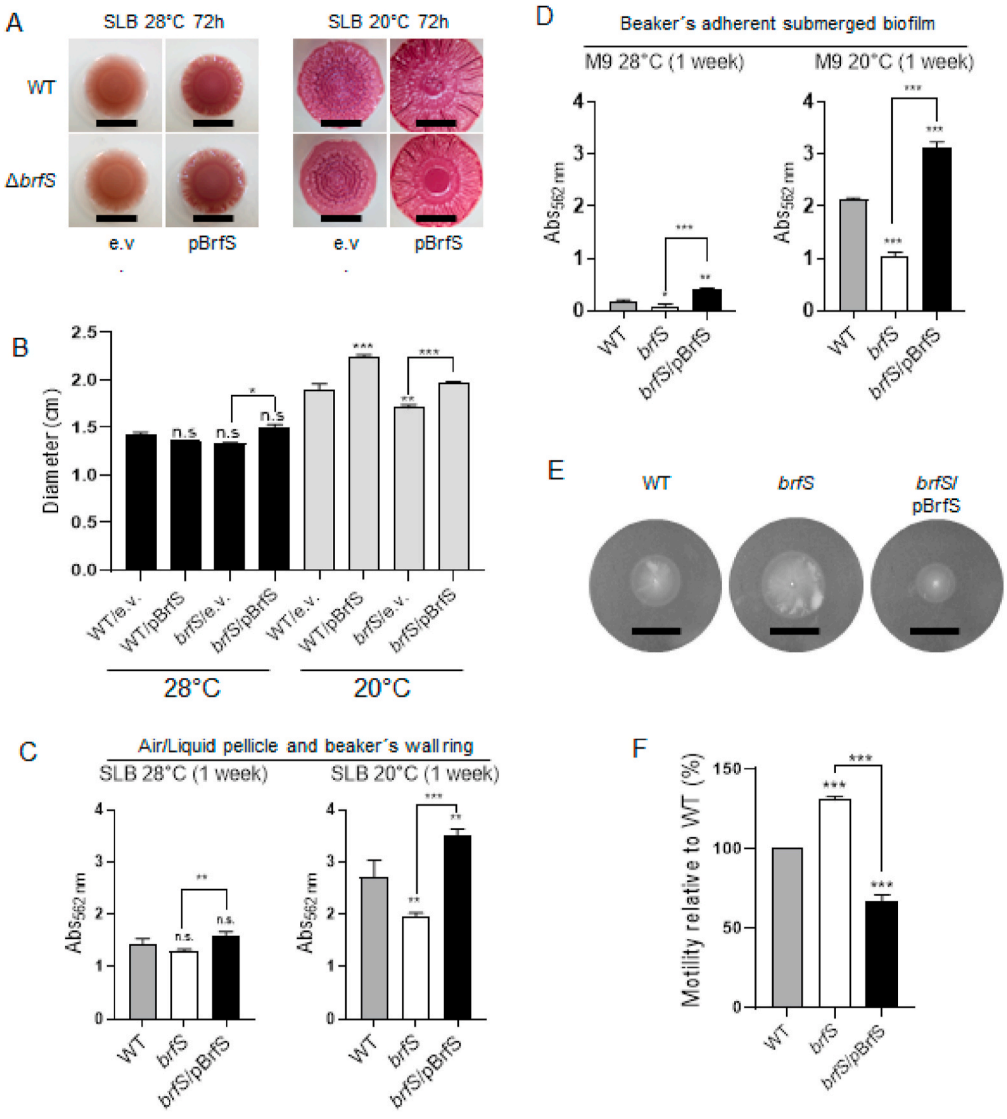

Fig. 2. BrfS controls biofilm formation and swimming motility at low temperatures. Wild-type, 14028s (WT), Δ*brfS*, Δ*brfS*/pBrfS, or a Δ*brfS*/pUHE21-2*laqI*^{q} (e.v.) cells were analyzed. (A, B) Red dry and rough (*rdar*) colony morphology (A) and size measurements (B) of the above-mentioned *S*. Typhimurium strains grown on CR agar plates at 28 °C or 20 °C for 72 h (Scale bars, 1 cm) (C, D) 1:100 dilutions of overnight LB cultures were incubated in SLB medium at 20 °C or 28 °C (C), or in M9 medium with glucose at 20 °C or 28 °C (D), for 1 week in borosilicate beakers without shaking. After successive washes, staining was performed with 1 % crystal violet and the absorbance at 562_{nm} was determined. (E, F) Swimming assay performed on SLB 0.3 % agar after 24 h of incubation at 20 °C, and its respective halo measurements. A) and E) are representative of experiments done at least three times (Scale bars, 2 cm). The data in the graphics correspond to average values of three independent experiments carried out by duplicate and the error bars represent *SD*. Symbols above bars denote statistical significance between means, with respect to WT or the indicated strains. n. s., not significant; *, $p < 0.05$; **, $p < 0.01$; ***, $p < 0.001$.

less wrinkled colonies on CR plates at 20 °C (Fig. 2A and B), and had substantially reduced air/liquid pellicles and adherent rings under static growth in rich liquid cultures at the low temperature (Fig. 2C and D, and Fig. S2) compared with the wild-type strain. The differences between the wild-type and the mutant strain were more evident when cells were grown in M9 with glucose at 20 °C (Fig. 2D), the condition for maximal BrfS and minimal MlrA expression (Fig. 1). It is noticeable that in this medium, the biomass is adhered to the bottom of the beaker instead of forming a ring in the interface (Fig. S2). Also, the overall amount of biofilm in the wild-type strain observed in this condition increased almost 10-fold compared with cells cultured at 28 °C (Fig. 2C). Similar biofilm phenotypes were observed using glass test tubes as abiotic surface (Fig. S2 E-H). (To note, the *rdar* phenotype did not develop on M9 minimal medium plates.)

BrfS overexpression from an IPTG-inducible low-copy number plasmid (pBrfS, Table S1), stimulated extracellular matrix production in both the wild-type and the Δ*brfS* mutant, particularly at 20 °C (Fig. 2A–D), resulting in large colonies with the typical *rdar* morphotype. The enhanced pEtN-cellulose production as a consequence of BrfS overexpression in the wild-type strain was also evidenced by staining the colonies with the dye Calcofluor (Fig. S3). Also, an increased swimming phenotype was observed in cells lacking *brfS* compared to wild-type cells, which was reverted by complementing with BrfS from the pBrfS plasmid (Fig. 2E and F). This suggests that, in addition to promoting biofilm production, BrfS suppresses flagellum-mediated motility to facilitate surface colonization.

We analyzed the BrfS-effect on CR plates at low temperature in mutant strains with impaired production of either curli (Δ*csgB*), cellulose (Δ*bcsA*), or both (Δ*csgD* or Δ*mlrA*) (Fig. 3). Slightly smaller colonies than those produced by the wild-type strain and with the typical *pdar* (pink dry and rough) morphotype [18] were observed in the Δ*csgB* strain that does not produce curli (Fig. 3). Further, deletion of *brfS* in this

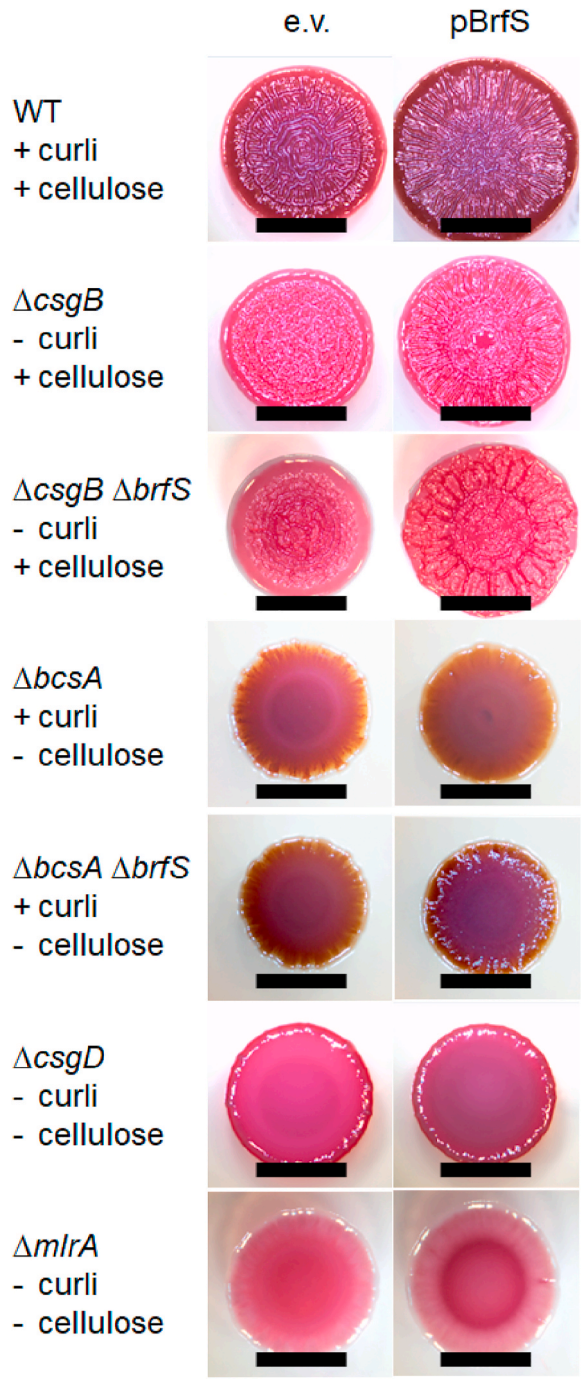

Fig. 3. Effect of BrfS on the *rdar* morphotype in different mutant strains affected in either curli or cellulose production. The figure shows the *rdar* colony morphology of the wild-type 14028s (WT), Δ*csgB*, Δ*csgB* Δ*brfS*, Δ*bcsA*, Δ*bcsA* Δ*brfS*, Δ*csgD* or the Δ*mlrA* strains and transformed either with an empty vector (e.v.) or with a plasmid expressing BrfS. The colonies were grown on Congo red agar at 20 °C without salt. (Scale bars, 1 cm).

mutant resulted in colonies with similar size, but with some morphological alterations. In particular, the edges of the colony became smoother and translucid. When BrfS was overexpressed in these cells, a modification in the wrinkle pattern was evident, indicating that even in the absence of curli, BrfS can alter the pEtN-cellulose disposition and/or distribution in the biofilm (Fig. 3).

The mutant in the cellulose synthase catalytic subunit coding gene, *bcsA*, showed the typical *bdar* (brown dry and rough) morphotype (Fig. 3) observed when only curli is present [18]. Overexpression of BrfS in this mutant did not exhibit significant modifications in colony morphology. A similar phenotype was observed in a strain lacking both *bcsA* and *brfS*. These results suggest that at 20 °C, cellulose is key for the formation of the proper *rdar* colony. Also, BrfS-mediated stimulation of matrix production was not observed in cells lacking either CsgD or MlrA, highlighting the importance of this regulatory cascade for biofilm production. Interestingly, the Δ*csgD* strain acquired a pink coloration at 20 °C (Fig. 3), in contrast to the almost white colony when grown at higher temperatures, i.e., 28-30 °C, on CR plates Fig. S4 and [18], suggesting that in this condition, a CsgD-independent pathway could residually activate some biofilm components.

2.3. Identification of genes under BrfS control

To elucidate the targets of BrfS regulation, we performed RNA-seq analysis comparing the transcriptional profile of the Δ*brfS* strain overexpressing BrfS from the pBrfS plasmid with the mutant strain carrying the empty vector (e.v.). Cells were grown overnight in M9 medium, at 23 °C in the presence of 250 μM IPTG. The genes whose expression changed significatively (false discovery rate [FDR], $\leq$0.01) by $\geq$ 3-fold between the Δ*brfS*/pBrfS and the Δ*brfS*/e.v. strains are listed in Table S4. We detected 151 genes whose expression was upregulated while 46 genes were downregulated by BrfS (Fig. 4A and Tables S4 and S5). The highest induction was observed for *csgB* and *csgA* (Fig. 4A and Fig. S5), encoding the minor and major curli subunit, respectively [35]. *csgC*, on the other hand, was not detected in the analysis. This is in agreement with previous observations that this gene is expressed at very low levels, contrary to *csgB* or *csgA*, and with the putative presence of a stem-loop structure between *csgA* and *csgC* that could account for *csgC* low transcription [36,37]. Furthermore, it also agrees with CsgC role in CsgA amyloid formation inhibition [20]. By contrast, minor or no significant BrfS-dependent activation was observed for the rest of the *csg* genes, encoding assembly/transport components or the regulatory protein CsgD required in much lower amounts than the structural components (Fig. S5). Similarly, not significant up-regulation for the genes involved in cellulose synthesis and transport was observed in the conditions tested.

BrfS-overexpression induced the transcription of a number of ribosomal-associated genes (Table S4), that could be related to a growth advantage of cells overexpressing BrfS. To test this, we compared the growth of the mutant and the complemented strain in liquid M9 medium at 20 °C (Fig. S6). Since no differences were observed, the reason of upregulation of the above-mentioned genes is not clear at this time. It also affected the transcription of genes linked to central metabolism (Table S4). For instance, genes involved in arginine/pyrimidine production (*car* and *arg*) and thiamine/purine biosynthesis (*thi* and *pur*) were induced by BrfS overexpression, while some genes related to histidine synthesis and iron uptake (*his* and *iro* operons) were repressed. The *STM14_3660-STM14_3661* operon was listed among the genes strongly repressed by BrfS-overexpression (Table S4). This operon encodes an Ail/OmpX-type outer membrane protein and its putative chaperone, which were reported to provide resistance to cephalosporins and to be part of the Cpx regulon [38,39]. This regulon is controlled by CpxR/CpxA, an envelope stress-responding two-component system, playing a role in modulating *Salmonella* biofilm formation under certain conditions [40]. Interestingly, *cpxP*, a gene encoding a CpxR/CpxA repressor, was also strongly downregulated by BrfS, while the *cpxA* gene coding for the histidine kinase of the system was induced (Table S4). The genes *rfbV*, *rfbN*, *rfbX* and *rfbU* involved in O-antigen capsule synthesis, another component of the extracellular matrix of *Salmonella* biofilms, were repressed as a consequence of BrfS expression.

To corroborate the RNA-seq results (Table S4), we selected some of the most affected genes and *bapA*, and compared their expression by qRT-PCR in cells overexpressing or not BrfS and grown under the conditions described above (Fig. S7). *bapA* encodes a large cell-surface protein that is part of the *Salmonella* extracellular biofilm matrix [41].

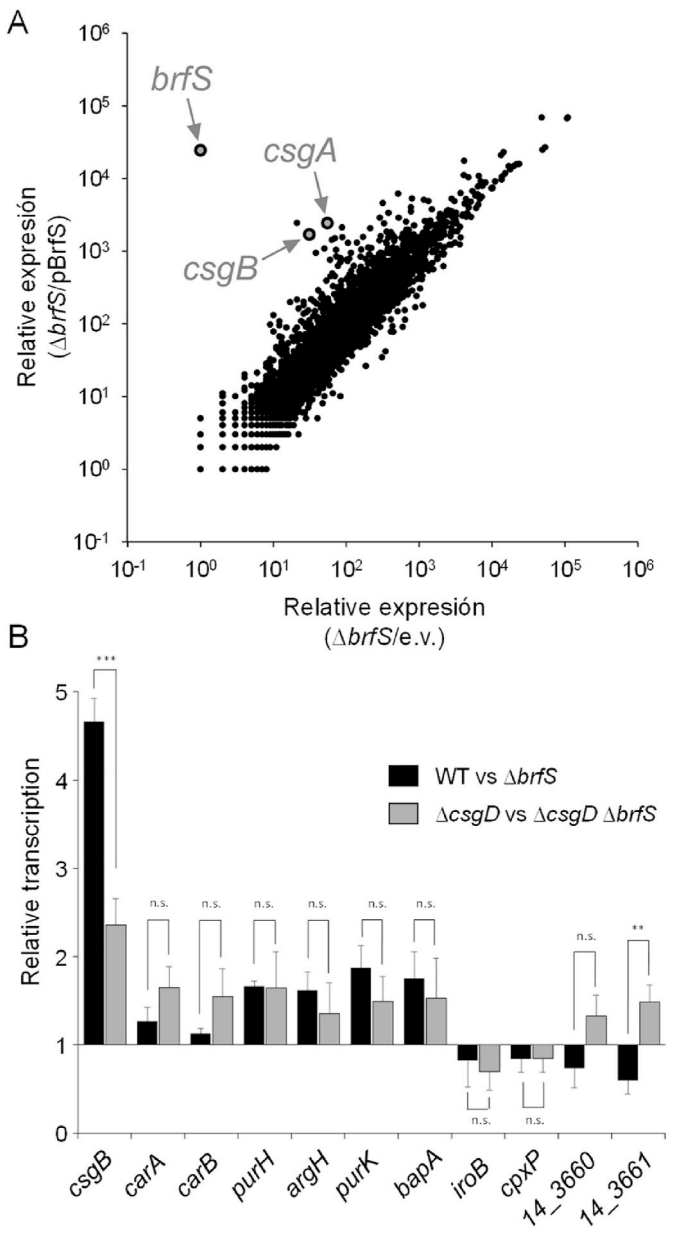

Fig. 4. RNA-seq analysis of *S.* Typhimurium Δ*brfS* strain without or with a plasmid expressing BrfS. (A) Scatter-plot showing relative RNA levels for all genes in Δ*brfS*/pBrfS or ΔbrfS/pUHE21-2*lacI*^{q} (e.v.) cells (see Tables S4 and S5). Each datapoint corresponds to a gene. The BrfS regulated genes *csgB* and *cgsA* are indicated. As a control, *brfS* is highlighted. (B) BrfS regulation of gene-transcription is exerted either through the canonical CsgD pathway or independent of CsgD. *csgB*, *carB*, *purH*, *argH*, *purK*, *carA*, *bapA*, *iroB*, *cpxP*, STM14_3660 and STM14_3661 gene expression analysis by qRT-PCR. The indicated cells were grown overnight at 20 °C in M9 medium with glucose. RNA quantitation and each gene relative transcription was performed as indicated in Materials and Methods. The y-axis represents the relative expression of each gene between the indicated strains. The data correspond to average values of three independent experiments carried out by duplicate and the error bars represent *SD*. Values below 1 indicates transcriptional repression. Symbols above bars denote statistical significance between means of the indicated strains. n. s., not significant; **, $p < 0.01$; ***, $p < 0.001$.

In the *S.* Typhimurium LT2 genome *bapA* is annotated as a pseudogene. Therefore, it was not listed in our RNA-seq dataset (Table S4). In spite of this, we observed an increase in the reads mapping at its mRNA in cells overexpressing BrfS by visual inspection of the *bapA* region (see Fig. S8A). BrfS-mediated regulation of this gene was corroborated using both qPCR (Fig. S7) and a chromosomal *bapA*:*lacZ* reporter (Fig. S8B). These results allowed us to propose BrfS as a *Salmonella* biofilm regulator that stimulates the synthesis of the extracellular matrix components at low temperatures.

2.4. BrfS induces curli transcription activation in a CsgD-dependent and independent manner

We compared the transcription pattern of selected genes either in the wild-type strain or its Δ*brfS* derivative (Fig. 4B) to analyze whether the BrfS-dependent regulation of these genes proceeds in cells expressing physiological levels of the regulator. The results correlated well with those presented in Fig. S7, although as expected, the levels of transcriptional modulation were lower than in cells overexpressing BrfS. This was particularly evident for *carB*, suggesting that the *car* operon is not a physiological target of BrfS.

We then investigated whether BrfS requires a functional CsgD to modulate transcription of *csgB* because its expression is known to depend on the canonical MlrA-CsgD induction cascade [24,41,42]. BrfS-mediated induction of *csgB* decreased in the Δ*csgD* background, but it was not abrogated (Fig. 4B). This suggests that BrfS can contribute to curli production both in a CsgD-dependent and independent manner. As with MlrA, BrfS can induce *csgD* transcription to modulate biofilm synthesis, and this is independent of the presence of MlrA (Fig. S9).

Our results also showed that the STM14_3661 gene, coding for an Ail/OmpX-like outer membrane protein involved ceftriaxone resistance [43], forms part of the BrfS-CsgD modulatory cascade because deletion of *csgD* abrogated the repression imposed by BrfS (Fig. 4B). No significant modulation was observed for STM14_3660, a periplasmic protein with putative chaperone-like activity that favors STM14_3661 activity [39] that was encoded in the same operon [43].

csgD deletion did not significantly affect the BrfS-dependent transcription of the rest of the analyzed genes, including *bapA*, suggesting CsgD-independent modulation of these BrfS targets.

2.5. BrfS-dependent induction of bapA at low temperature does not require the MrlA-CsgD cascade

The use of a *bapA*:*lacZ* reporter in *S.* Typhimurium strains deleted for *brfS*, *csgD* or both allowed us to confirm that BrfS-dependent expression of *bapA* does not requires CsgD to activate this gene at low temperature (Fig. 5A). This differs from the CsgD-dependent expression of *bapA* reported in *S.* Enteritidis [9]. In fact, BrfS-dependent transcription of *bapA*, both under physiological conditions or when BrfS was overexpressed, was not affected by the deletion of *mlrA* (Fig. 5B). Western-blot analysis allowed us to corroborate the MlrA-, MlrB-independent, BrfS-dependent regulation of BapA expression (Fig. 5C), indicating that in *S.* Typhimurium and at least under the conditions tested, *bapA* is not integrated into the canonical MlrA-CsgD cascade.

Altogether, these results indicate that BrfS is a *Salmonella*-specific MrlA-like regulator able to modulate expression of a series of genes including those required for extracellular matrix production at low temperatures.

3. Discussion

Salmonella biofilm formation is a complex and highly regulated process, involving multiple transcription factors responding to different intracellular signals. This allows this pathogen to survive and persist not only inside the host but also in the environment. Previously, we showed that MlrB, an MlrA homolog, contributes to *Salmonella* virulence by repressing *csgD* transcription and biofilm formation inside host cells [32]. In this work, we characterize another MlrA homolog, the *Salmonella*-specific BrfS transcription factor (Fig. S1). We demonstrate its importance for *Salmonella* biofilm formation at low temperatures and in nutrient-deprived media (Figs. 2 and 3). *brfS* transcription is stimulated

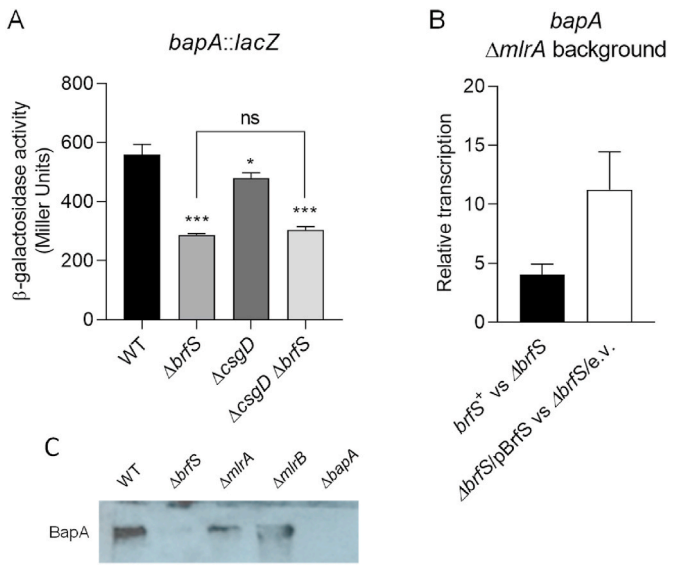

Fig. 5. BrfS controls BapA expression. (A) β-galactosidase activity determined in extracts from the wild-type or the indicated mutant strains carrying the *bapA*:*lacZ* transcriptional reporter. Cells were grown in M9 medium + glucose at 20 °C with shacking. Values are means and SD of three independent experiments performed in duplicates. Symbols above bars denote statistical difference between means of the wild-type and the mutant except when it is indicated. n. s., not significant; *, $p < 0.05$; ***, $p < 0.001$. (B) Quantitative real-time PCR performed to compare *bapA* transcription between the Δ*mlrA* and the Δ*mlrA* Δ*brfS* strains, or between the Δ*mlrA* Δ*brfS* harboring the pBrfS plasmid and the Δ*mlrA* Δ*brfS* carrying the empty vector (e.v.). Cells were grown as describe in Fig. 4. The y-axis represents the fold induction. (C) Western blot analysis of BapA in the indicated strains using anti-BapA antibodies. Whole-cell extracts were prepared from stationary-phase cultures grown as indicated in materials and methods.

in these conditions, in contrast to the *mlrA* expression (Fig. 1).

Based on the conservation of the DNA-binding site region between BrfS and MlrA (Fig. S1), we predicted that BrfS would control biofilm production by inducing *csgD* transcription. Nevertheless, the results presented here show that BrfS-controlled gene expression is much more complex than this, and that there are genes modulated by BrfS that either follow of the canonical MlrA-CsgD regulation or they are independent of this pathway. BrfS-dependent transcription of *csgD* was not evident in the RNA-seq analysis (Table S4), but was detected through quantitative real-time PCR experiments in cells deleted of *mlrA* (Fig. S9). Although CsgD is required for maximal BrfS-mediated transcriptional activation of the curli structural genes, some BrfS-dependent activation occurs in the absence of the LuxR-like regulator. Furthermore, BrfS-activation of another biofilm component, *bapA*, does not require CsgD (Figs. 4 and 5). Whether BrfS recognizes the *bapA* or the *csgD* promoters is a matter of future investigations because, despite multiple attempts, we have so far been unable to purify BrfS in its active form.

In a previous report, Kao et al. [34] showed that BrfS activates the transcription of *csgD* and *csgA*, but it does not influence the production of cellulose. Nevertheless, their studies were all performed at 25 °C in static liquid cultures and using rich growth media. Thus, these experimental conditions differ from the maximal BrfS-expression conditions that we showed in this report. In addition, Kao et al. [34] were unable to detect extracellular matrix production in the mutant deleted for *brfS*, while in our case, we only observed differences between the wild-type and Δ*brfS* strains when working at 20 °C (Fig. 2). On the other hand, they reported that although BrfS is expressed at low temperatures and must be involved in non-host linked biofilms, the Δ*brfS* strain exhibited an attenuated virulence in a mice model. Nevertheless, we were unable to replicate this phenotype in a competition assay using the Streptomycin-treated mice model (our unpublished results). The nature of the abiotic surfaces tested, difference in growth conditions, or virulence model could account for these discrepancies. Again, our results strongly support the integration of BrfS into the canonical MlrA-CsgD activation pathway for biofilm formation as deletion of either the curli-biosynthetic genes or the genes coding for the production of pEtN-cellulose affect the BrfS-stimulated phenotype on CR plates (Fig. 3).

3.1. Metabolic alterations triggered by BrfS

Our transcriptomic studies revealed that BrfS stimulates the expression of genes involved in purine or pyrimidine biosynthesis (Fig. 4). The products of the *pur* genes are involved in the synthesis of precursors for c-di-GMP formation, a second messenger that is essential for biofilm formation [28]. Also, activation of these genes and those involved in pyrimidine biosynthesis could enhance the production and secretion of extracellular DNA, another well-known component of the *Salmonella* biofilm matrix [13]. This is supported by a number of reports that link the genes involved in nucleotide biosynthetic pathways with the production and balance of curli and cellulose in biofilms from different bacterial species [44–46].

The most strongly repressed genes by BrfS in our transcriptomic analysis were *STM14_3661* and *STM14_3660*, that are linked to cephalosporin resistance [39]. They integrate an operon described as part of *Salmonella* CpxRA regulon [47], but their regulation has not been completely elucidated. These genes are reported to be repressed by the CpxA kinase but induced by the response regulator CpxR [47]. These observations agree with our results showing that BrfS activates *cpxA* and strongly inhibits *cpxP* transcription (Table S4), which may result in CpxA activation and a further repression of the *STM14_3661-STM14_3660*. In addition, we noticed that the BrfS-mediated repression of *STM14_3661* is lost in cells lacking *csgD* (Fig. 4). Because CpxR/CpxA also influences *csgD* expression, the link between BrfS, CsgD and the Cpx regulon, may require further investigation.

In sum, our results show that BrfS controls *Salmonella* biofilm formation at low temperatures. This suggests that BrfS can contribute to *Salmonella* persistence when the pathogen is facing nutrient deprivation in low temperature environments. It may even favor the conditions to form biofilms and colonize vegetable tissues, ensuring its subsequent dissemination to new hosts [22]. Overall, this provides an example of how *Salmonella* relies on various regulatory factors to finely control the type and amount of biofilm matrix components required to thrive in specific environments.

4. Experimental procedures

4.1. Bacterial strains and growth conditions

S. enterica serovar Typhimurium derivative strains and plasmids used in this study are listed in Table S1. Oligonucleotides are listed in Table S2. Cells were grown at 37 °C, 30 °C, 28 °C or 20 °C in Luria–Bertani without NaCl (SLB) or in M9 medium [48] supplemented with sterile-filtered glucose as a carbon source to reach a final concentration of 0.4 % (w/v). Ampicillin, kanamycin, and chloramphenicol were used, when necessary, at a final concentration of 100, 50, and 20 μg/ml, respectively. All reagents and chemicals were from Sigma, except the Luria Bertani and M9 minimal salts culture media that were from Difco. Oligonucleotides were purchased from Macrogen, Inc. Enzymes were purchased from New England Biolabs, Promega or Life Technologies.

4.2. Construction plasmids and strains

The strains carrying gene deletions or chromosomal lacZ reporter fusions, were generated by Lambda Red-mediated recombination

followed by P22-mediated transduction using previously described protocols [49–52]. When necessary, antibiotic resistance cassettes inserted at the deletion sites were removed using FLP-mediated recombination [53]. DNA fragments as well as plasmids were introduced into bacterial cells by electroporation. All constructs were verified by DNA sequencing.

To obtain the expression plasmid pPB1407 (Table S1), the gene encoding *bfrS* was PCR amplified from *Salmonella* Typhimurium 14028s chromosome using the brfS fw BamHI NdeI/ brfS rv HindIII primer pair (Table S2), and the Q5® High-Fidelity DNA Polymerase (New England Biolabs). The PCR products were treated with *Bam*HI and *Hind*III, and cloned into pUH21-2*laqI*^{q} (Table S1) digested with the same enzymes.

4.3. Quantification of biofilm adhesion to abiotic surfaces

To evaluate the adhesion to polystyrene microplates, a Crystal Violet (CV) binding and quantification protocol was implemented [54]. For this, 1:100 dilutions of saturated cultures of the tested strains (grown in the presence of 250 μM of IPTG) were deposited in borosilicate beakers (final volume of 20 ml) or glass test tubes (final volume of 5 ml), which were incubated at the temperatures and times indicated. After incubation, the supernatants were discarded and the beakers or tubes were washed four times with distilled water and allowed to dry at room temperature. Then, 20 or 5 ml of a 1 % (w/v) aqueous solution of CV was added to the beakers or to the test tubes respectively, and incubated for 20 min at room temperature. Subsequently, unbound CV was washed out thoroughly with distilled water. After drying the plates at room temperature, an ethanol: acetone mixture 80:20 (v/v) was added to each beaker or tube. Desorption of the dye was allowed for 1 h at room temperature on a shaking platform. Finally, the absorbance at 562 nm was recorded using a spectrophotometer (BioTek ELχ808).

4.4. Rdar morphotype

The rdar morphotype was judged visually on Congo red (CR) agar plates. Five microliters of a saturated bacterial cultured grown in LB ($OD_{600\ nm}$ of 5.0) were spotted onto SLB agar plates supplemented with Congo red (40 mg/l) and Coomassie brilliant blue G-250 (20 mg/l), and 250 μM of IPTG when needed. Plates were incubated at the temperatures and times indicated and development of the colony morphology and color was analyzed.

4.5. Cellulose qualitative assay

Qualitative assessment of bacterial cellulose production was determined on calcofluor agar plates. Five microliters of a saturated bacterial culture grown in LB ($OD_{600\ nm}$ of 5) were spotted onto SLB agar plates supplemented with 50 μg/mL calcofluor white (fluorescent brightener 28, Sigma) and with 250 μM of IPTG. Plates were incubated at 20 °C or 28 °C for 72 h, and fluorescence was observed under a UV light source.

4.6. β-galactosidase activity assays

Measurements of β-galactosidase activity of strains carrying transcriptional fusions to the *lacZY* genes were made following a modification of the protocol proposed by Miller [55], and essentially as described by [51]. 250 μM of IPTG were added to the culture medium when needed.

4.7. Protein extraction and western blot analysis

For protein extraction, 1 mL of culture of each strain was grown overnight in M9 at 20 °C. After cell lysis and separation of the soluble fraction, protein concentration was quantified using the BCA kit (Thermo Scientific) to apply the same amount in the SDS-PAGE. Western blot was carried out as described previously [51,56], using rabbit polyclonal anti-BapA antibodies (generously provided by Dr. Iñigo Lasa; Universidad Pública de Navarra, Pamplona, Spain).

4.8. Swimming motility assay

To test swimming motility, 5 ml of an overnight culture ($OD_{600\ nm}$ = 5) was inoculated into SLB medium containing 0.3 % agar with or without 250 μM IPTG. The swimming halos were observed after 24 h at 20 °C.

4.9. RNA-seq

Overnight cultures of 14028s Δ*brfS*/pUH21-2*laqIq* (CDS114) and 14028s Δ*brfS*/pBrfS (CDS115) were grown overnight at 37 °C in LB supplemented with 100 μg/mL ampicillin with shaking at 225 rpm. M9 minimal medium (1X M9 minimal salts, 2 mM $MgSO_4$, 0.1 mM $CaCl_2$) was prepared and supplemented with 0.4 % glucose, 100 μg/mL ampicillin, and 250 μM IPTG. Overnight cultures were washed twice with the prepared M9 minimal medium, diluted 1:40 in the M9 minimal medium, and grown at 23 °C with shaking at 200 rpm until the $OD_{600\ nm}$ reached 1.15–1.35. RNA was purified from cells as described previously [57]. RNA was treated with Turbo DNase (Invitrogen) according to the manufacturer's protocol. rRNA removal and library construction were performed as described previously [57]. Sequencing was performed by the Advanced Genomics Technologies Core at the Wadsworth Center on a NextSeq 1000 Instrument. Sequence reads were aligned to the *S.* Typhimurium 14028s reference genome using Rockhopper [58].

4.10. RNA isolation and analysis of gene expression by qRT-PCR

The strains to be tested were grown overnight in M9 liquid medium, with or without 250 μM IPTG at 20 °C. RNA extraction was done as described by [59]. Total RNA samples were treated with RQ1 RNase-free DNase I (Promega). The integrity of the RNA samples was checked by agarose electrophoresis. First-strand cDNA was synthesized with MoMLV-reverse transcriptase (Promega) following the manufacturer's instructions, using 2 μg RNA and random primers. Relative expression was determined by performing quantitative real-time PCR in an Accurate 96 Real-Time PCR System (DLAB), using the HOT FIREPol® EvaGreen® qPCR Mix Plus (ROX) (Solis BioDyne) with primers listed in Table S2. A 10-fold dilution of cDNA obtained as described above was used as template. Samples containing no reverse transcriptase or template RNA were included as negative controls to ensure RNA samples were free of DNA contamination. Cycling parameters were as follows: initial denaturation at 95 °C for 12 min; 40 cycles of 95 °C for 10 s, 60 °C for 20 s and 72 °C for 20 s; and a final extension of 72 °C for 10 min. Results are informed using the $2^{-\Delta\Delta CT}$ method [60], using *gapdH* gene as a housekeeping gene. Each cDNA sample was run in technical triplicate and repeated in at least three independent sets of samples.

4.11. Comparative protein analysis and construction of the phylogenetic tree

The protein sequences of the MlrA-like regulators used in the alignment and in the phylogenetic tree were downloaded from NCBI Table S3 and [31]. Sequences were aligned by ClustalW algorithm, and a maximum likelihood phylogenetic tree was constructed using MEGA X.

4.12. Statistical analysis

To test for statistical differences between means, one-way analysis of variance (ANOVA) and the Tukey multiple-comparison test with an overall significance level of 0.05 were used. Calculations were performed with GraphPad Prism statistical software.

CRediT authorship contribution statement

Gonzalo Tulin: Writing – original draft, Methodology, Investigation, Formal analysis, Conceptualization. **Andrea A.E. Méndez:** Validation, Resources, Investigation, Formal analysis. **Nicolás R. Figueroa:** Methodology, Investigation, Conceptualization. **Carol Smith:** Resources, Methodology, Investigation. **María P. Folmer:** Investigation. **Diego Serra:** Writing – original draft, Validation, Methodology, Formal analysis. **Joseph T. Wade:** Writing – original draft, Validation, Supervision, Software, Methodology, Investigation, Funding acquisition, Formal analysis, Data curation. **Susana K. Checa:** Writing – original draft, Visualization, Validation, Resources, Project administration, Methodology, Investigation, Formal analysis, Conceptualization. **Fernando C. Soncini:** Writing – review & editing, Writing – original draft, Supervision, Project administration, Funding acquisition, Formal analysis, Conceptualization.

Declaration of competing interest

The authors declare the following financial interests/personal relationships which may be considered as potential competing interests. Fernando C. Soncini reports financial support was provided by National Agency for the Promotion of Research Technological Development and Innovation. Joseph T. Wade reports financial support was provided by National Institutes of Health. If there are other authors, they declare that they have no known competing financial interests or personal relationships that could have appeared to influence the work reported in this paper.

Acknowledgments

This work was supported by grants from Agencia Nacional de Promoción Científica y Tecnológica (ANPCyT) (PICT-2019-2019-00982; PICT-2018-02122) to FCS, and by The National Institutes of Health grant 1R35GM144328 to JTW. AAEM is postdoctoral fellow of CONICET. MPF is recipient of a doctoral fellowship from ANPCyT. DOS, SKC and FCS are career investigators of CONICET. FCS is also a Career Investigator of the Consejo de Investigaciones de la Universidad Nacional de Rosario. SKC, AAEM, NRF and DOS are Faculty members of the Facultad de Ciencias Bioquímicas y Farmacéuticas, Universidad Nacional de Rosario.

Appendix A. Supplementary data

Supplementary data to this article can be found online at https://doi.org/10.1016/j.bioflm.2025.100254.

Data availability

Data will be made available on request.

References

[1] Eng S-K, Pusparajah P, Ab Mutalib N-S, Ser H-L, Chan K-G, Lee L-H. *Salmonella*: a review on pathogenesis, epidemiology and antibiotic resistance. Front Life Sci 2015;8:284–93.
[2] Billah MM, Rahman MS. *Salmonella* in the environment: a review on ecology, antimicrobial resistance, seafood contaminations, and human health implications. J Hazardous Mater Adv 2024;13:100407.
[3] Maruzani R, Sutton G, Nocerino P, Marvasi M. Exopolymeric substances (EPS) from *Salmonella enterica*: polymers, proteins and their interactions with plants and abiotic surfaces. J Microbiol 2019;57:1–8.
[4] Waldner LL, MacKenzie KD, Köster W, White AP. From exit to entry: long-term survival and transmission of *Salmonella*. Pathogens 2012;1:128–55.
[5] Branchu P, Bawn M, Kingsley RA. Genome variation and molecular epidemiology of *Salmonella enterica* serovar typhimurium pathovariants. Infect Immun 2018;86. https://doi.org/10.1128/iai.00079-00018.
[6] Simm R, Ahmad I, Rhen M, Le Guyon S, Romling U. Regulation of biofilm formation in *Salmonella enterica* serovar Typhimurium. Future Microbiol 2014;9:1261–82.
[7] Römling U, Bian Z, Hammar M, Sierralta WD, Normark S. Curli fibers are highly conserved between *Salmonella typhimurium* and *Escherichia coli* with respect to operon structure and regulation. J Bacteriol 1998;180:722–31.
[8] Römling U, Sierralta WD, Eriksson K, Normark S. Multicellular and aggregative behaviour of *Salmonella typhimurium* strains is controlled by mutations in the *agfD* promoter. Mol Microbiol 1998;28:249–64.
[9] Latasa C, Roux A, Toledo-Arana A, Ghigo J-M, Gamazo C, Penadés JR, Lasa I. BapA, a large secreted protein required for biofilm formation and host colonization of *Salmonella enterica* serovar Enteritidis. Mol Microbiol 2005;58:1322–39.
[10] Solano C, Garcia B, Valle J, Berasain C, Ghigo JM, Gamazo C, Lasa I. Genetic analysis of *Salmonella enteritidis* biofilm formation: critical role of cellulose. Mol Microbiol 2002;43:793–808.
[11] Ledeboer NA, Jones BD. Exopolysaccharide sugars contribute to biofilm formation by *Salmonella enterica* serovar typhimurium on HEp-2 cells and chicken intestinal epithelium. J Bacteriol 2005;187:3214–26.
[12] Crawford RW, Gibson DL, Kay WW, Gunn JS. Identification of a bile-induced exopolysaccharide required for *Salmonella* biofilm formation on gallstone surfaces. Infect Immun 2008;76:5341–9.
[13] Wang H, Huang Y, Wu S, Li Y, Ye Y, Zheng Y, Huang R. Extracellular DNA inhibits *Salmonella enterica* serovar typhimurium and S.enterica serovar typhi biofilm development on abiotic surfaces. Curr Microbiol 2014;68:262–8.
[14] Evans ML, Chapman MR. Curli biogenesis: order out of disorder. Biochim Biophys Acta Mol Cell Res 2014;1843:1551–8.
[15] Serra DO, Richter AM, Hengge R. Cellulose as an architectural element in spatially structured *Escherichia coli* biofilms. J Bacteriol 2013;195:5540–54.
[16] Römling U, Rohde M, Olsén A, Normark S, Reinköster J. AgfD, the checkpoint of multicellular and aggregative behaviour in *Salmonella typhimurium* regulates at least two independent pathways. Mol Microbiol 2000;36:10–23.
[17] Hammar Mr, Arnqvist A, Bian Z, Olsén A, Normark S. Expression of two csg operons is required for production of fibronectin- and Congo red-binding curli polymers in *Escherichia coli* K-12. Mol Microbiol 1995;18:661–70.
[18] Zogaj X, Bokranz W, Nimtz M, Römling U. Production of cellulose and curli fimbriae by members of the family *Enterobacteriaceae* isolated from the human gastrointestinal tract. Infect Immun 2003;71:4151–8.
[19] Bhoite S, van Gerven N, Chapman MR, Remaut H. Curli biogenesis: bacterial amyloid assembly by the type VIII secretion pathway. EcoSal Plus 2019;8. https://doi.org/10.1128/ecosalplus.ESP-0037-2018.
[20] Evans Margery L, Chorell E, Taylor Jonathan D, Åden J, Götheson A, Li F, Koch M, Sefer L, Matthews Steve J, Wittung-Stafshede P, Almqvist F, Chapman Matthew R. The bacterial curli system possesses a potent and selective inhibitor of amyloid formation. Mol Cell 2015;57:445–55.
[21] Gerstel U, Römling U. The csgD promoter, a control unit for biofilm formation in *Salmonella typhimurium*. Res Microbiol 2003;154:659–67.
[22] Cowles KN, Willis DK, Engel TN, Jones JB, Barak JD. Diguanylate cyclases AdrA and STM1987 regulate *Salmonella enterica* exopolysaccharide production during plant colonization in an environment-dependent manner. Appl Environ Microbiol 2016;82:1237–48.
[23] Gibson DL, White AP, Snyder SD, Martin S, Heiss C, Azadi P, Surette M, Kay WW. *Salmonella* produces an O-antigen capsule regulated by AgfD and important for environmental persistence. J Bacteriol 2006;188:7722–30.
[24] Brown PK, Dozois CM, Nickerson CA, Zuppardo A, Terlonge J, Curtiss R. MlrA, a novel regulator of curli (AgF) and extracellular matrix synthesis by *Escherichia coli* and *Salmonella enterica* serovar Typhimurium. Mol Microbiol 2001;41:349–63.
[25] Newman SL, Will WR, Libby SJ, Fang FC. The curli regulator CsgD mediates stationary phase counter-silencing of *csgBA* in *Salmonella* Typhimurium. Mol Microbiol 2018;108:101–14.
[26] Sokaribo AS, Hansen EG, McCarthy M, Desin TS, Waldner LL, MacKenzie KD, Mutwiri G, Herman NJ, Herman DJ, Wang Y, White AP. Metabolic activation of CsgD in the regulation of *Salmonella* biofilms. Microorganisms 2020;8:964.
[27] Hengge-Aronis R. Signal transduction and regulatory mechanisms involved in control of the σ^S (RpoS) subunit of RNA Polymerase. Microbiol Mol Biol Rev 2002;66:373–95.
[28] Serra DO, Hengge R. A c-di-GMP-Based switch controls local heterogeneity of extracellular matrix synthesis which is crucial for integrity and morphogenesis of *Escherichia coli* macrocolony biofilms. J Mol Biol 2019;431:4775–93.
[29] Tschowri N, Busse S, Hengge R. The BLUF-EAL protein YcgF acts as a direct anti-repressor in a blue-light response of Escherichia coli. Genes Dev 2009;23:522–34.
[30] Tschowri N, Lindenberg S, Hengge R. Molecular function and potential evolution of the biofilm-modulating blue light-signalling pathway of Escherichia coli. Mol Microbiol 2012;85:893–906.
[31] Tulin G, Figueroa NR, Checa SK, Soncini FC. The multifarious MerR family of transcriptional regulators. Mol Microbiol 2024;121:230–42.
[32] Echarren ML, Figueroa NR, Vitor-Horen L, Pucciarelli MG, Garcia-Del Portillo F, Soncini FC. Balance between bacterial extracellular matrix production and intramacrophage proliferation by a *Salmonella*-specific SPI-2-encoded transcription factor. Mol Microbiol 2021;116:1022–32.
[33] Pontes MH, Lee E-J, Choi J, Groisman EA. *Salmonella* promotes virulence by repressing cellulose production, vol. 112. Proceedings of the National Academy of Sciences; 2015. p. 5183–8.
[34] Kao S, Serfecz J, Sudhakar A, Likosky K, Romiyo V, Tursi S, Tükel Ç, Wilson JW. *Salmonella enterica* serovar Typhimurium STM1266 encodes a regulator of curli biofilm formation: the *brfS* gene. FEMS (Fed Eur Microbiol Soc) Microbiol Lett 2023;370.
[35] Tursi SA, Tükel Ç. Curli-containing enteric biofilms inside and out: matrix composition, immune recognition, and disease implications. Microbiol Mol Biol Rev 2018;82. https://doi.org/10.1128/mmbr.00028-00018.

[36] Barnhart MM, Chapman MR. Curli biogenesis and function. Annu Rev Microbiol 2006;60:131–47.
[37] Collinson SK, Clouthier SC, Doran JL, Banser PA, Kay WW. Salmonella enteritidis agfBAC operon encoding thin, aggregative fimbriae. J Bacteriol 1996;178:662–7.
[38] Huang H, Sun Y, Yuan L, Pan Y, Gao Y, Ma C, Hu G. Regulation of the two-component regulator CpxR on aminoglycosides and β-lactams resistance in *Salmonella enterica* serovar typhimurium. Front Microbiol 2016;7.
[39] Lin Y-H, Yang T-C, Hu WS. Characterization of *stm3030* and *stm3031* genes of *Salmonella enterica* serovar Typhimurium in relation to cephalosporin resistance. J Microbiol Immunol Infect 2019;52:282–8.
[40] Shetty D, Abrahante JE, Chekabab SM, Wu X, Korber DR, Vidovic S. Role of CpxR in biofilm development: expression of key fimbrial, O-antigen and virulence operons of *Salmonella enteritidis*. Int J Mol Sci 2019;20:5146.
[41] Jonas K, Tomenius H, Kader A, Normark S, Römling U, Belova LM, Melefors Ö. Roles of curli, cellulose and BapA in *Salmonella* biofilm morphology studied by atomic force microscopy. BMC Microbiol 2007;7:70.
[42] Ogasawara H, Yamamoto K, Ishihama A. Regulatory role of MlrA in transcription activation of *csgD*, the master regulator of biofilm formation in *Escherichia coli*. FEMS (Fed Eur Microbiol Soc) Microbiol Lett 2010;312:160–8.
[43] Hu WS, Lin JF, Lin YH, Chang HY. Outer membrane protein STM3031 (Ail/OmpX-like protein) plays a key role in the ceftriaxone resistance of Salmonella enterica serovar Typhimurium. Antimicrob Agents Chemother 2009;53:3248–55.
[44] Cepas V, Ballén V, Gabasa Y, Ramírez M, López Y, Soto SM. Transposon insertion in the purL gene induces biofilm depletion in *Escherichia coli* ATCC 25922. Pathogens 2020;9:774.
[45] Garavaglia M, Rossi E, Landini P. The pyrimidine nucleotide biosynthetic pathway modulates production of biofilm determinants in *Escherichia coli*. PLoS One 2012;7:e31252.
[46] Gélinas M, Museau L, Milot A, Beauregard PB. The *de novo* Purine Biosynthesis Pathway Is the Only Commonly Regulated Cellular Pathway during Biofilm Formation in TSB-Based Medium in *Staphylococcus aureus* and *Enterococcus faecalis*. Microbiol Spectr 2021;9.
[47] Jing W, Liu J, Wu S, Li X, Liu Y. Role of *cpxA* mutations in the resistance to aminoglycosides and β-lactams in *Salmonella enterica* serovar typhimurium. Front Microbiol 2021;12.
[48] Sambrook J, Russell DW. Molecular cloning: a laboratory manual. third ed. Cold Spring Harbor Laboratory Press; 2001.
[49] Ibanez MM, Cerminati S, Checa SK, Soncini FC. Dissecting the metal selectivity of MerR monovalent metal ion sensors in Salmonella. J Bacteriol 2013;195:3084–92.
[50] López C, Checa SK, Soncini FC. CpxR/CpxA controls *scsABCD* transcription to counteract copper and oxidative stress in *Salmonella enterica* serovar typhimurium. J Bacteriol 2018;200.
[51] Perez Audero ME, Podoroska BM, Ibanez MM, Cauerhff A, Checa SK, Soncini FC. Target transcription binding sites differentiate two groups of MerR-monovalent metal ion sensors. Mol Microbiol 2010;78:853–65.
[52] Pezza A, Pontel LB, Lopez C, Soncini FC. Compartment and signal-specific codependence in the transcriptional control of Salmonella periplasmic copper homeostasis. Proc Natl Acad Sci U S A 2016;113:11573–8.
[53] Datsenko KA, Wanner BL. One-step inactivation of chromosomal genes in Escherichia coli K-12 using PCR products. Proc Natl Acad Sci U S A 2000;97:6640–5.
[54] Pitts B, Hamilton MA, Zelver N, Stewart PS. A microtiter-plate screening method for biofilm disinfection and removal. J Microbiol Methods 2003;54:269–76.
[55] Miller JH. Experiments in molecular genetics. NY: Cold Spring Harbor; 1972.
[56] Pontel LB, Soncini FC. Alternative periplasmic copper-resistance mechanisms in Gram negative bacteria. Mol Microbiol 2009;73:212–25.
[57] Stringer AM, Currenti S, Bonocora RP, Baranowski C, Petrone BL, Palumbo MJ, Reilly AA, Zhang Z, Erill I, Wade JT. Genome-scale analyses of Escherichia coli and Salmonella enterica AraC reveal noncanonical targets and an expanded Core regulon. J Bacteriol 2014;196:660–71.
[58] McClure R, Balasubramanian D, Sun Y, Bobrovskyy M, Sumby P, Genco CA, Vanderpool CK, Tjaden B. Computational analysis of bacterial RNA-Seq data. Nucleic Acids Res 2013;41.
[59] Ramírez MS, Müller GL, Pérez JF, Golic AE, Mussi MA. More than just light: clinical relevance of light perception in the nosocomial pathogen acinetobacter baumannii and other members of the genus acinetobacter. Photochem Photobiol 2015;91:1291–301.
[60] Livak KJ, Schmittgen TD. Analysis of relative gene expression data using real-time quantitative PCR and the $2-\Delta\Delta CT$ method. Methods 2001;25:402–8.